Evaluating Reforestation Techniques in Arid Regions of Kenya and Tanzania through Remote Sensing

Yenny Paola Betancur-Torres*, Ixent Galpin

Universidad de Bogota-Jorge Tadeo Lozano, Bogota, Colombia

Abstract

This paper analyzes changes in vegetation in areas of Kenya and Tanzania resulting from the reforestation activities of Justdiggit. These activities involve digging semicircles in the ground, with and without sowing grass seeds, to retain rainwater and promote soil infiltration for plant uptake. In this study, remote sensing techniques are employed to calculate variations in the NDVI, SAVI, and NDWI indices. Additionally, supervised machine learning models, including SVM, Random Forest, and Decision Trees, are trained to quantify changes in vegetation cover from satellite images. These images, sourced from the LandSat 8 satellite collections, are processed in Google Earth Engine. The analysis spans three years prior to the reforestation activities up to 2022 to illustrate the changes.

The results analysis considers soil cover, the SAVI index, precipitation, and the climatic seasonality of the area. On average, the reforestation method with grass seed sowing increased the SAVI index by 0.06 and the percentage of vegetation cover by 3.39%. Conversely, the reforestation method without sowing decreased the SAVI index by 0.04 but increased the percentage of vegetation cover by 9.04%. It is concluded that the technique with grass seed sowing produces better results compared to the semicircle technique without sowing. However, the prolonged drought in the area significantly impacted the observed results.

Keywords

Reforestation, Remote Sensing, Satellite Imagery, Vegetation Index, Machine Learning

1. Introduction

Global warming and climate change are established facts supported by various studies [1, 2]. All humans have contributed to the gradual intensification of these phenomena [3, 4, 5]. While global warming primarily results from increased atmospheric concentrations of greenhouse gases, it also indirectly impacts plant life. In some regions, soil degradation and loss of productive capacity due to erosion have been observed [2]. Countries like Tanzania and Kenya in Africa are particularly affected by droughts [6, 7]. The soil in these regions is arid and compact, causing rainwater to run off the surface without being absorbed. Consequently, crops and vegetation do not receive adequate water, leading to low food production and high temperatures that adversely affect the population [8].

Fortunately, some organizations are actively working to counteract global warming. One such organization is Justdiggit, a foundation that has been re-greening and restoring degraded areas in Kenya and Tanzania in recent years. This restoration helps lower temperatures locally and globally [8]. Justdiggit employs nature-based techniques to restore ecological balance. One of their methods involves digging semi-circles in the ground, both with and without planting grass seeds. These semi-circles act as natural dams, retaining rainwater and allowing it to penetrate the soil, creating a favorable environment for grassland growth. The roots of these grasslands further retain water and help decompact the soil, fostering an environment that supports insect life. These insects, in turn, pollinate plants, thus sustaining natural cycles and revitalizing the soil. These restoration efforts positively impact biodiversity, water security, and food security for local inhabitants [8].

This work focuses on measuring the outcomes of Justdiggit's activities in Kenya and Tanzania, initiated between 2016 and 2021. The study evaluates changes in vegetation according to the reforestation

ICAIW 2024: Workshops at the 7th International Conference on Applied Informatics 2024, October 24–26, 2024, Viña del Mar, Chile
*Corresponding author.
yenny.betancurt@utadeo.edu.co (Y. P. Betancur-Torres); ixent@utadeo.edu.co (I. Galpin)
0009-0000-5908-4200 (Y. P. Betancur-Torres); 0000-0001-7020-6328 (I. Galpin)

techniques applied to identify the most efficient methods. Remote sensing techniques and machine learning models are employed to identify and classify areas with vegetation from the beginning of these projects until 2022. The input data consists of multispectral satellite images captured by the Landsat 8 Satellite [9]. These images allow us to analyze changes in the study areas based on reflectance, using each beam of light to detect variations in the terrain.

This paper builds on previous work [10] to quantify the vegetation changes resulting from Justdiggit's activities in Kenya and Tanzania using satellite imagery. It applies supervised machine learning and remote sensing techniques to analyze data from the beginning of the projects until 2022, aiming to determine the most effective reforestation techniques. The specific contributions are:

- Collecting a set of multispectral satellite images with less than 20% cloud cover for each study area where reforestation took place between 2016 and 2021, from the start of each project until 2022.
- Generating spectral indices and manually labeling samples of the area types at the pixel level, which will be used to train and evaluate the machine learning models.
- Training and evaluating supervised classification models (Decision Trees, Random Forest, and SVM) to identify the best-performing model for classifying land cover.
- Applying the best-performing model to classify vegetated soils in the study areas.
- Analyzing the information obtained from the classification models and indices.
- Identifying the most effective reforestation techniques applied in the study areas.

This work employs the CRISP-DM methodology, which comprises six stages [11].

This article has the following structure: Section 2 describes the vegetation spectral indices and satellite image-related techniques used in this work. Section 3 reviews research on similar topics, providing the foundation for the present study. Section 4 defines the areas under study, the satellite image sources, and the minimum criteria that must be met. Section 5 defines the training polygons for the models and generates the indices necessary to capture the training points. Using the images selected in the previous phase, supervised classification models (Decision Trees, Random Forest, and SVM) are generated and evaluated to identify the best model for classifying vegetation and non-vegetation areas. Subsequently, we use the selected model to classify the pixels in the images, determining the vegetation area in each study area on an annual basis. Section 6 analyzes the classified data along with the indices information to determine the more effective reforestation method. Finally, Section 7 presents the conclusions.

2. Preliminaries

This project utilizes satellite images captured by remote sensors. These images are multispectral, containing reflectance data of the surface across different bands. Each band provides numerical values at the pixel level, and when these bands are combined, they reveal valuable information [12]. In Landsat 8, bands 2, 3, and 4 (Red, Green, and Blue) are combined to produce images close to true or natural color. However, combining bands 3, 4, and 5 highlights healthy vegetation in red [13].

Spectral vegetation indices are crucial for highlighting phenomena such as changes in vegetation, achieved by combining specific bands [14]. The normalized difference vegetation index (NDVI) helps identify the density and health of plant masses [15]. The NDVI is calculated using the following formula, which employs the near-infrared (NIR) and red (Red) bands [16]:

$$NDVI = (NIR - Red)/(NIR + RED) \tag{1}$$

The Soil Adjusted Vegetation Index (SAVI) allows the identification of plant masses, similar to the NDVI, but with the advantage of minimizing the influence of bare soil brightness using a correction factor L. This makes SAVI ideal for identifying changes in vegetation in the areas under study [17]. The formula uses the near-infrared (NIR) and red (Red) bands [17]:

$$SAVI = \frac{NIR - Red}{NIR + Red + L} * (1 + L) \quad (2)$$

The Normalized Difference Water Index (NDWI) is suitable for identifying water bodies [18]. Its formula uses the NIR and Green bands [19]:

$$NDWI = (Green - NIR)/(Green + NIR) \quad (3)$$

3. Related Work

Several studies have investigated deforestation using satellite images. Early works include Bezanilla *et al.* [20], who examined forest degradation and recovery in the Sierra Fría in Mexico, and Armenteras *et al.* [21], who analyzed the dynamics and causes of deforestation in Latin American forests, reviewing 283 articles. More recently, Ariza [22] used maximum likelihood models and regression models to determine which index best highlighted the effects of vegetation burning caused by fires in central Spain, using remote sensing of soils. García *et al.* [23] focused on identifying Ecuadorian forests, which experienced a 15% decrease between 1990 and 2020 due to logging driven by the expansion of agricultural land in the Zapotal river basins. They used remote sensing techniques and vegetation indices to conduct their analysis.

Satellite image analysis is also used to identify other trends. For example, Medina *et al.* [24] analyzed the loss of glacial volume in the Parón mountain range in the Peruvian Andes using Landsat satellite images. They used the snow index (NDSI) from 1987 to 2011, identifying an average glacial decrease of 18%. Similarly, Veettil *et al.* [25] studied the behavior of glaciers in the Tropical Andes using remote sensing techniques, revealing a rapid retreat of these glaciers since 1970. Sánchez *et al.* [26] applied remote sensing techniques to identify and monitor biodiversity patterns and the influence of human activities on these changes at both local and global levels. Serra *et al.* [27] utilized remote sensing techniques and index calculations to characterize the geomorphology and lava pulses of the Aguas Calientes volcano and its surroundings in the Tinogasta department of Argentina. Valcarce [28] applied machine learning techniques in remote sensing for crop monitoring, using images obtained from synthetic aperture radar (SAR) sensors regardless of weather conditions.

Liang *et al.* [29] compared deep learning techniques with the maximum likelihood algorithm to satellite image classification methods in China, identifying the most optimal approach. Ramírez *et al.* [30] detected land cover changes using the Random Forest algorithm applied to satellite images combined with drone-captured images. Alvarado *et al.* [31] studied the change in agricultural extension in the Yarada de los Palos district in Peru from 2000 to 2020, using multispectral satellite images and remote sensing techniques, finding a 265.84% increase in agricultural areas. Mejía *et al.* [32] evaluated water erosion in an area of Tacna in Peru, training models and calculating indices. Rahal *et al.* [33] mapped clayey soils in northwestern Algeria using ASTER satellite images to establish soil mineralogy. Estrada *et al.* [34] identified the biomass of grasslands in a high Andean plant community in Peru. Finally, Ahman *et al.* [35] discussed the importance of artificial intelligence in teaching plant physiology, emphasizing its role in complementing remote sensing for disease detection, yield prediction, and simulation generation, among other applications.

There is previous work investigating Justdiggit's activities. Steele *et al.* [36] investigated vegetation growth in the Kuku area of Kenya using VanderSat remote satellites. Similarly, Villani identified vegetation changes in Dodoma, Tanzania, where Justdiggit has also been conducting reforestation activities [37]. On the other hand, van der Vliet *et al.* [38] applied remote sensing techniques to identify soil water retention and temperature changes in two areas of Tanzania. These works are different from our work, as they study vegetation changes prior to 2021. In addition, they do not compare the efficiency of the two techniques used, *i.e.*, whether spreading grass seeds improves reforestation.

4. Data Acquisition and Preprocessing

Justdiggit kindly provided via email the type of reforestation, year of start of activities and number of semicircles in each area, and a KML (Keyhole Markup Language) file with the location and area of the polygons in which Justdiggit has carried out reforestation activities in Tanzania and Kenya[1].

Justdiggit currently operates in Tanzania, Kenya, Uganda, and Ethiopia, with activities initiated between 2016 and 2022. However, this project focuses solely on activities in Tanzania and Kenya that began between 2016 and 2021 [8]. Areas where activities started in 2022 are excluded due to the insufficient time to observe significant changes in vegetation. In Kenya and Tanzania, Justdiggit has carried out reforestation activities using two methods in different areas, which are described below:

- Semicircles of soil without planting: This method involves digging semicircles into the soil against the slope of the land. These semicircles act as natural dams, retaining rainwater and allowing it sufficient time to penetrate the soil, thereby enabling natural vegetation growth [8].
- Semicircles of soil with sowing: This method, like the previous method, consists of digging semicircles in the soil against the slope and additionally spreading grass seeds [8], of the species "African Foxtail" and "Maasai Lovegrass"[2].

In data exploration, the Normalized Difference Vegetation Index (NDVI) is generated for the images of each study area to measure the density and health of the vegetation. The images are captured from three years before the start of reforestation activities until 2022, aiming to identify trends in vegetation changes during this period. According to the World Bank, Kenya and Tanzania experience seasonal variations with months of more rain and others being drier [39, 40], which is reflected in the NDVI, as it increases during months with higher rainfall. This is consistent with observations that wet and dry seasons in the tropics affect plant growth similarly to how seasons do in temperate regions [41]. To reduce variability caused by climatic seasonality, images are selected from the consecutive dry months of June and July, allowing for better annual comparisons while minimizing cloudiness and lost pixels. Additionally, images from three years before the start of reforestation until 2022 are analyzed to assess changes in vegetation due to these activities.

4.1. Selection of Satellite Images

Satellite images are obtained from Google Earth Engine (GEE)[3], which offers a vast catalog of satellite images and geospatial data. GEE also provides online data processing on its servers, free for academic and research purposes [42]. From these satellite images, indices are calculated to highlight land cover characteristics [16], aiding in the capture of training points that form the training dataset for supervised machine learning models. These images are also used to apply the selected supervised machine learning model.

A collection of satellite images is selected in GEE considering several important criteria. Firstly, the temporal aspect is crucial, as information from 2013 to 2022 is needed to analyze vegetation changes before and after Justdiggit's reforestation activities. Additionally, it is ensured that the images include the spectral bands necessary to calculate indices and capture training points for machine learning models, as well as to analyze vegetation changes. The images are also verified for rectification to avoid inconsistencies in the data. Finally, the spatial resolution of the images is considered, with a preference for high resolution to obtain more precise details in each pixel.

It is observed that the collections from the Landsat 7 and 8 satellites meet the defined conditions. However, the Landsat 7 satellite sensor experienced a scan line corrector failure in May 2003, resulting in images with gaps that correspond to a loss of approximately 25% of the data [43]. Therefore, the collection of images captured by the Landsat 8 satellite, which does not present this issue, is selected for the development of this project.

[1] T. Zaan [Personal communication]. September 22, 2023.
[2] T. Zaan [Personal Communication]. September 22, 2023.
[3] https://earthengine.google.com/

4.2. Preparation of Satellite Images

For the development of this project, the Landsat 8 Collection 2 available on GEE is used. Several preprocessing steps are performed on these images as suggested by GEE [44]. First, value scaling is applied, as the original images are in integers, with a scale factor of 2.75e-05 and an offset of -0.2 for Landsat 8 [9, 44]. Next, the images are cropped to include only the information relevant to each study area. Cloud masking is applied using the QA_PIXEL band to remove pixels affected by clouds or cloud shadows, which could distort the data [9, 44, 45]. Finally, to address the issue of missing pixels after cloud masking, a composite of images from the same weather station is created. This is achieved by applying the 'reducer' aggregation function on the median of images from each year within the same season, minimizing changes in the ground surface [45].

Images undergo value scaling, cropping, and cloud masking processes. Additionally, a median shrinking function is used to create composite images from June 1 to July 31 of each year, resulting in one composite image per year for each study area. The full satellite images, covering approximately 170 km x 183 km, may have scene overlap and varying percentages of cloud cover [9]. However, this percentage refers to the entire image and not to the specific study area. Therefore, the percentage of cloud cover in each study area is determined by the number of missing pixels after applying the preparation processes. Images with more than 20% cloud cover are discarded, as this level of cloud cover significantly interferes with the investigation due to the considerable loss of information [46].

5. Model Training and Evaluation for Land Cover Classification

Two training iterations of the soil classification models are performed. In the first iteration, detailed in [10], a polygon covering most of the Chyulu (Kuku) National Park in southern Kenya is defined for model training. This area was chosen because it includes a variety of land covers: vegetation, agriculture, urbanization, and water bodies. Training points are obtained from indices applied to the area, and tests are conducted for the categories *vegetation*, *soil*, *water*, *urban*, and *agriculture*. Three supervised machine learning models are used to classify the coverage of the study areas: Support Vector Machines (SVM), Decision Trees, and Random Forest. The SVM model, using default hyperparameters, exhibited errors in classifying urban areas and water bodies, and failed to correctly identify the agriculture category. Decision Trees, also with default hyperparameters, showed similar issues but managed to identify some agricultural pixels incorrectly. The Random Forest model, trained with 100 trees, provided a more accurate classification of vegetation and soil compared to the SAVI index, but also made errors in classifying urban areas, water bodies, and agricultural areas.

In the second iteration, a larger training polygon is chosen, covering more areas where Justdiggit has carried out reforestation activities in southern Kenya. This polygon is shown in Figure 1. The months of June and July 2020, corresponding to the dry season, are selected for this capture. Only vegetation and soil cover points are captured, considering that the areas where Justdiggit conducted reforestation activities do not correspond to urban or agricultural areas, and water bodies are excluded from the training polygon. To capture these points, the SAVI index with a correction factor of 0.5 is used, resulting in the visualization shown in Figure 2(a), generated from the composite image of Landsat 8. The values are displayed in a color range from brown to green, where brown represents soil and green represents vegetation. A total of 2253 points are captured, comprising 1124 vegetation points and 1129 soil points.

After capturing the points, the training image data is extracted, using the band values corresponding to the pixels of these points in the composite image of June and July 2020. The data is then partitioned, with 70% for training and 30% for testing. Figure 2 shows the classification obtained for the three classification models used.

For the Support Vector Machine (SVM) model, shown in Figure 2(b), the "Margin" decision procedure is applied to set a margin between the target classes, and the "Linear Kernel" is selected so that the model uses a linear function for classification. The other hyperparameters are left at their default settings. To train the decision tree model, the hyperparameters were set to a minimum population of 40

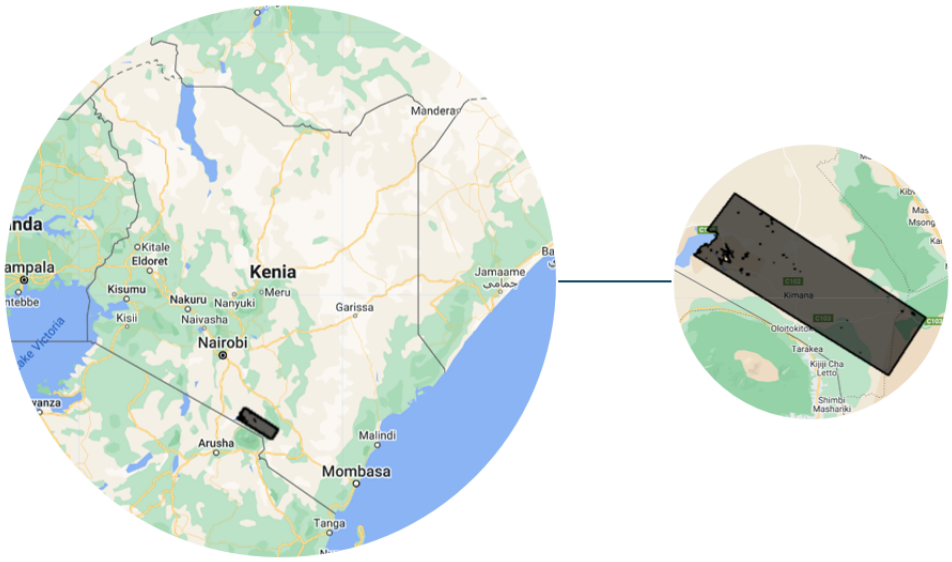

Figure 1: Training polygon, plotted using Google Earth Engine [47].

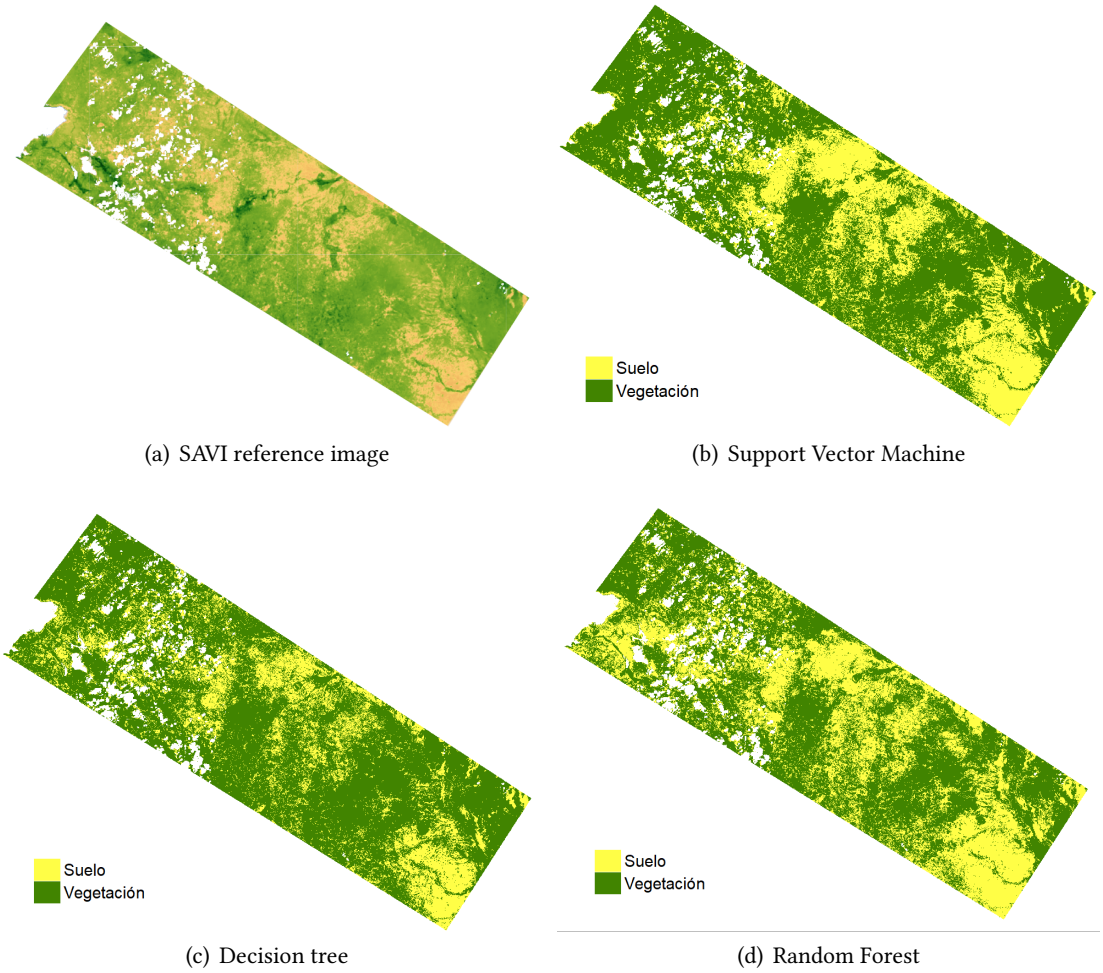

(a) SAVI reference image

(b) Support Vector Machine

(c) Decision tree

(d) Random Forest

Figure 2: Reference Image vs. Classification obtained from the trained models

points per node and a maximum of 80 nodes. This configuration was used for data classification, and the results are presented in Figure 2(c). Finally, the classification performed by the random forest model

is shown in Figure 2(d).

To determine whether the models are generalizing well, and to identify if they are overfitting or underfitting [48], the cross-validation method is used with five folds and iterations for each model. Additionally, the average and variance of their accuracies are calculated. The results are presented in Table 1. The SVM model shows the best performance, as it has the highest average accuracy and the smallest variance. This indicates that the accuracies of the iterations do not differ significantly, suggesting that the SVM model is generalizing better compared to the other two models.

Table 1
Classification accuracy results obtained using cross-validation ($k = 5$)

Fold	SVM	Decision tree	Random Forest
1	0.9869	0.9475	0.9540
2	0.9803	0.9694	0.9301
3	0.9868	0.9430	0.9605
4	0.9861	0.9769	0.9446
5	0.9821	0.9576	0.9420
Mean	0.9845	0.9589	0.9462
Variance	0.000009147	0.000205135	0.000136407

6. Comparative Analysis

In this phase, firstly, the SVM model, which has demonstrated superior performance, is applied to identify the soil and vegetation cover in the areas under study. The detailed results for each polygon are presented in [10].

For the analysis of the results, the following factors are taken into account:

- *Areas with vegetation*: The application of the model determines the percentage of vegetation and soil cover in the study areas.
- *The SAVI index*: This index allows the identification of vegetation density and health by minimizing the influence of bare soil brightness. The scale ranges from -1 to 1, where negative values or values close to zero represent surfaces without vegetation, and positive values represent vegetation cover. The closer the value is to 1, the denser the vegetation [17].
- *Precipitation*: This factor is included in the analysis, considering that vegetation in this part of Africa is affected by climatic seasonality and the amount of precipitation in the study areas [41]. Since 2019, East Africa has been experiencing water shortages due to lack of rain, even during seasons that typically see higher rainfall [49, 50]. This drought, classified by the UNHCR as the worst in the last 40 years [50], significantly affects the results of Justdiggit's reforestation efforts, making it an important part of the analysis. Information on monthly accumulated rainfall is obtained from the dataset published by the University of Idaho, measured in millimeters (mm), indicating liters of rain per square meter [51]. For this study, the average accumulated rainfall for June and July of each year is used.

It is worth noting that all polygons have experienced a significant and prolonged decrease in rainfall since 2019, as shown in Figure 3. Considering this and the fact that the polygons were reforested in different years, which can cause variations in the results, a comparison is made between the results of polygons reforested in the same year but with different techniques.

6.1. Polygons Reforested in 2018

In 2018, reforestation activities were conducted in the Pembamoto and Nasipa polygons. Pembamoto was reforested with grass seed sowing, while Nasipa was reforested without sowing grass seeds. Figure 4

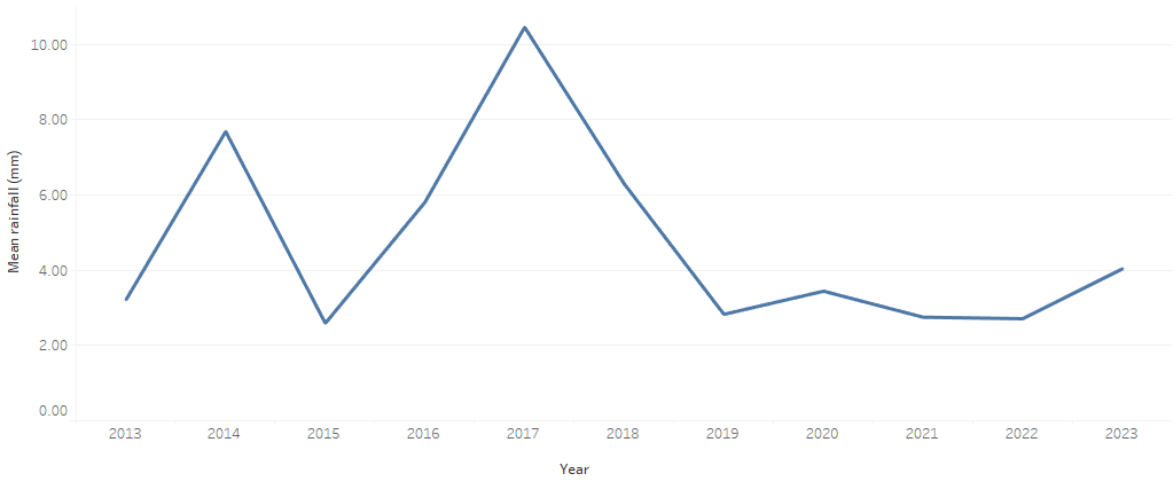

Figure 3: Average rainfall for all polygons

contrasts the rainfall results. Despite missing information for two years, it is generally observed that Nasipa received more rainfall than Pembamoto.

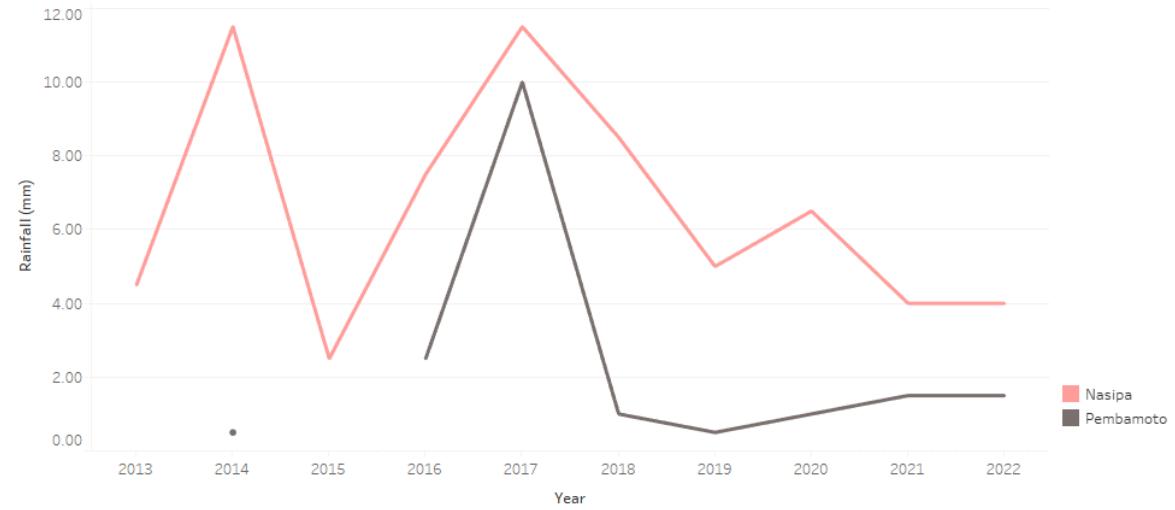

Figure 4: Comparison of rainfall in polygons reforested in 2018

Figure 5 compares the vegetation cover percentages. Despite missing data for one year after reforestation, it is generally observed that Pembamoto had a higher percentage of vegetation cover than Nasipa from 2018 onwards.

Figure 6 compares the SAVI index results. Despite missing data for one year after reforestation, it is generally observed that Pembamoto had a higher SAVI index than Nasipa from 2018 onwards.

The averages of the results before and after reforestation for each polygon, shown in Tables 2 and 3, are compared to identify whether the changes were positive or negative. It is observed that the polygon with grass seed sowing had better results in the annual comparison of the variables' percentage of vegetation and SAVI, despite experiencing less rainfall. When comparing the difference in average results before and after reforestation, it is noted that although Pembamoto had a decrease in the percentage of vegetation cover, it showed a greater increase in the SAVI index with less rainfall compared to Nasipa. Based on these observations, it is concluded that in 2018, the technique of reforesting with soil semicircles and grass seed sowing yielded better results.

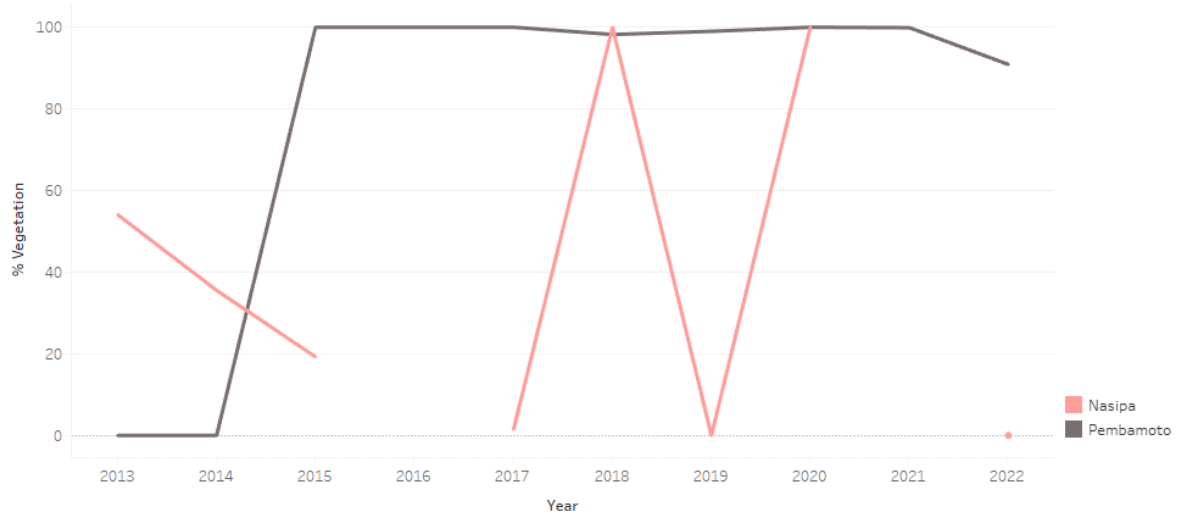

Figure 5: Comparison of vegetation percentage of polygons reforested in 2018

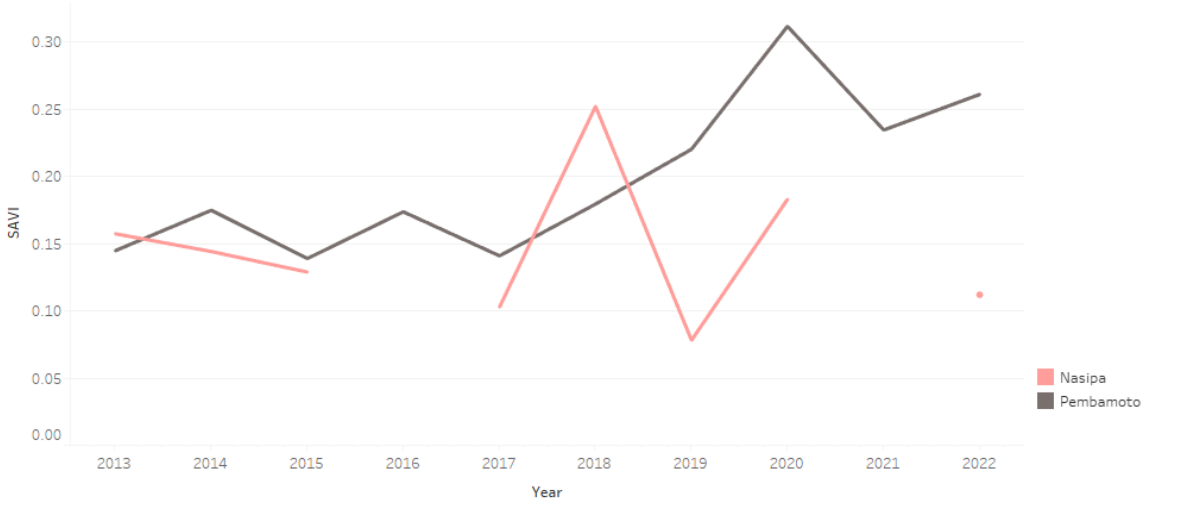

Figure 6: Comparison of the SAVI index of polygons reforested in 2018

6.2. Polygons Reforested in 2019

In 2019, reforestation activities were carried out in the Enkii, KukuA, and Risa polygons. Enkii was reforested with sowing, while KukuA and Risa were reforested without sowing grass seeds. Figure 7 contrasts the rainfall results. Despite missing information for one year, it is generally observed that Enkii received more rainfall than Risa and KukuA.

Figure 8 compares the results of vegetation cover percentage. Despite missing data in the years following 2019, it is generally observed that Risa had a higher percentage of vegetation cover than Enkii and KukuA after reforestation. Additionally, Enkii had greater vegetation coverage than KukuA.

Figure 9 compares the results of the SAVI index. Despite missing data in the years following 2019, it is generally observed that Enkii had a higher SAVI index than KukuA and Risa after reforestation.

However, when comparing the difference in average results before and after reforestation for each polygon, it is evident that Enkii had an increase in the percentage of vegetation cover and SAVI index despite receiving less rainfall compared to Risa and KukuA. Based on these observations, it is concluded that in 2019, the technique of reforesting with soil semicircles and grass seed sowing yielded better results.

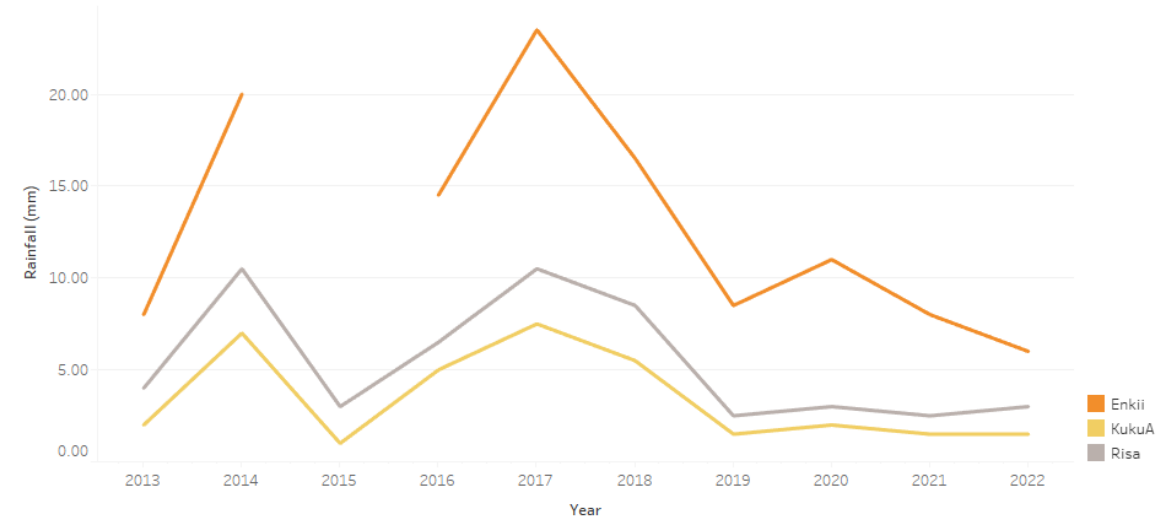

Figure 7: Comparison of rainfall in polygons reforested in 2019

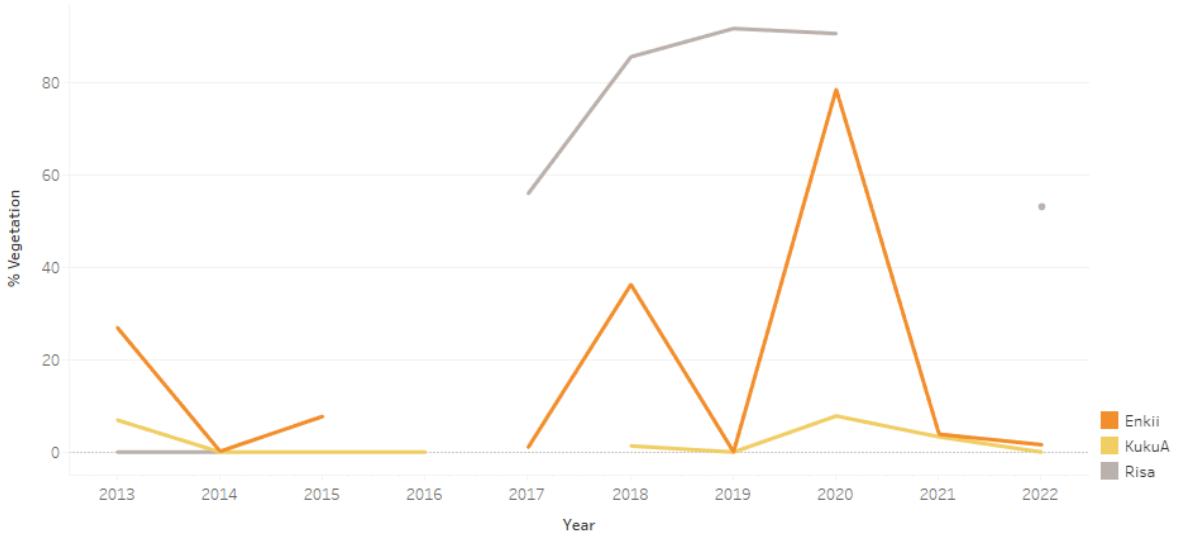

Figure 8: Comparison of vegetation percentage of polygons reforested in 2019

6.3. Discussion

The averages of the results before and after reforestation for each polygon, as shown in Tables 2 for 2018, and Table 3 for 2019, are compared to determine the nature of the changes, whether positive or negative. Table 4 summarizes the difference in results according to the sowing technique. The tables show that the polygons that underwent reforestation with grass seed sowing showed better results in the annual comparison of the three variables: percentage of vegetation cover and SAVI, although it experienced higher rainfall.

7. Conclusion

The objective of this work is to determine which of the reforestation techniques implemented by Justdiggit in areas of Kenya and Tanzania is most effective. These techniques involve digging semicircles in the ground, with and without sowing seeds, in study areas where reforestation began between

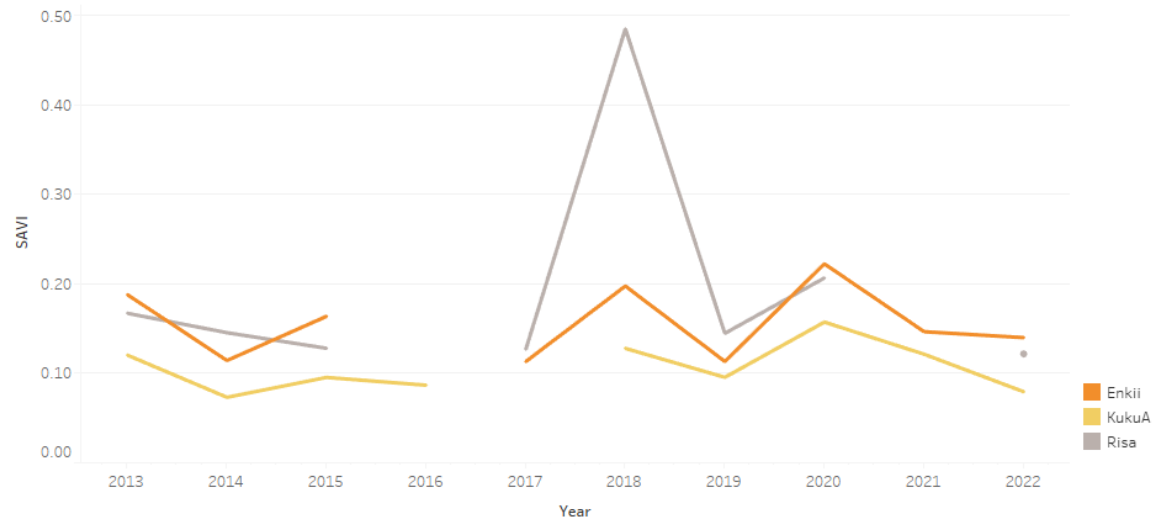

Figure 9: Comparison of the SAVI index of polygons reforested in 2019

Table 2
Difference in Average Results of Reforestation of Semicircles planted in 2018

Polygon	Technique	Percentage vegetation	SAVI	Rainfall
Nasipa	without sowing	22.96	0.0085	-1.833
Pembamoto	with sowing	-2.56	0.1057	-5.13
Mean		10.2	0.06	-3.48

Table 3
Difference in Average Results of Reforestation of Semicircles planted in 2019

Polygon	Technique	Percentage vegetation	SAVI	Rainfall
Enkii	with sowing	9.34	0.0142	-11.70
Risa	without sowing	1.11	-0.1418	-6.5
KukuA	without sowing	3.04	0.0120	-3.583
Mean		4.50	-0.04	-7.26

Table 4
Difference in Average Results of Reforestation of Semicircles by Technique

Technique	Percentage vegetation	SAVI	Rainfall
without sowing	9.03667	-0.04043	-3.971
with sowing	3.39	0.05995	-8.415
Difference	-5.64667	0.100383	-4.444

2016 and 2021. To conduct this analysis, remote sensing, and supervised machine learning techniques are applied to quantify the change in vegetation caused by Justdiggit's activities from the start of the reforestation projects until 2022. It is determined that for the polygons reforested in 2018 and 2019, the method with grass seed sowing increased the SAVI index by an average of 0.06 and the percentage of vegetation cover by 3.39%. In contrast, the method without sowing decreased the SAVI

index by 0.04 but increased the percentage of vegetation cover by 9.04%. This demonstrates that both methods are effective, but the technique with grass seed sowing yields better results compared to the semicircle technique without sowing. It is also concluded that rainfall is a critical factor in the success of reforestation, as both methods' outcomes were influenced by the prolonged drought in the Horn of Africa.

Future work would benefit from using images with higher spatial resolution and less cloud cover, as well as conducting on-site verification of land cover at the training points. Additionally, it would be beneficial to extend the study period to include more years, so as to include polygons reforested en 2021-2022, allowing for a more comprehensive demonstration of the vegetation evolution in the reforested areas.

Acknowledgments

We would like to thank Thijs van der Zaan from Justdiggit for providing information about the polygons in the study area. We also express our sincere gratitude to Liliana Castillo and Rodrigo Gil from the Faculty of Agrarian Sciences at the National University of Colombia for their invaluable insights and guidance, which greatly contributed to the interpretation of satellite imagery in this study.

References

[1] L. R. Brown, El Mundo Al Borde Del Abismo, Cómo Evitar el Declive Ecológico y el Colapso de la Economía : Ensayo Ecológico y Económico., 1st ed. ed., Centro de Estudios para el Desarrollo Sostenible, 2015.

[2] J. A. Alonso, El Planeta Tierra en peligro : calentamiento global, cambio climático, soluciones, Club Universitario, 2013.

[3] J. M. Urtaza, Cambio climático y patógenos en el agua: el fenómeno de el niño y su impacto en la salud, Revista de salud ambiental 11 (2011).

[4] E. F. Labarca, El lado oculto del cambio climático y el calentamiento global, RIL editores, 2020.

[5] I. Gough, Calentamiento Global, Codicia y Necesidades Humanas: Cambio Climático, Capitalismo y Bienestar Sostenible, 1 ed., Miño y Dávila Editores, 2023.

[6] E. N. Service, Más de 9 millones de personas en riesgo de hambre por sequía en sur de África: África sequÍa, 2019. URL: https://www.proquest.com/docview/2299489875?pq-origsite=primo&sourcetype=Wire%20Feeds.

[7] E. N. Service, Onu pide a países donantes más ayudas para combatir sequía en cuerno África: Onu África, 2011.

[8] Justdiggit, Justdiggit | cooling down the planet | global warming charity, 2023. URL: https://justdiggit.org/.

[9] G. LLC, S. G. de EE. UU, Usgs landsat 8 level 2, collection 2, tier 1 earth engine data catalog google for developers, 2024. URL: https://developers.google.com/earth-engine/datasets/catalog/LANDSAT_LC08_C02_T1_L2.

[10] Yenny Paola Betancur Torres, Analisis Temporal de los Métodos de Reforestración Aplicados por JustDiggit en Áreas de Kenia y Tanzania Mediante Imágenes Satelitales, Master's thesis, Universidad de Bogotá Jorge Tadeo Lozano, 2024.

[11] P. Chapman, CRISP-DM 1.0: Step-by-step Data Mining Guide, SPSS, 2000. URL: https://books.google.com.co/books?id=po7FtgAACAAJ.

[12] J. A. J. A. Richards, X. Jia, Remote sensing digital image analysis: an introduction, 2 ed., Springer, 1993. doi:10.1007/978-3-662-03978-6.

[13] M. Gonzalez, E. Mendoza, Introducción a la teledetección sesión 2, 2019. URL: https://appliedsciences.nasa.gov/sites/default/files/EO4IM_Session_2_Espanol.pdf.

[14] C. S. E. de Romaní, Estudio de índices de vegetación a partir de imágenes aéreas para la detección

de déficit hídrico y aplicaciones en la agricultura de precisión y en la evaluación de daños en seguro agrario del almendro, en parcela de 20 ha en chiloeches (guadalajara) (2022).

[15] R. P. Gupta, Remote Sensing Geology, 3rd ed. 2018. ed., Springer Berlin / Heidelberg, 2017. doi:10.1007/978-3-662-55876-8.

[16] P. M. Mather, M. Koch, Computer Processing of Remotely-Sensed Images: An Introduction, fourth edition ed., John Wiley I& Sons, Incorporated, 2011. doi:10.1002/9780470666517.

[17] A. Huete, A soil-adjusted vegetation index (savi), Remote sensing of environment 25 (1988) 295–309. doi:10.1016/0034-4257(88)90106-X.

[18] B. cai Gao, Ndwi—a normalized difference water index for remote sensing of vegetation liquid water from space, Remote sensing of environment 58 (1996) 257–266. doi:10.1016/S0034-4257(96)00067-3.

[19] F. Cigna, H. Xie, Imaging Floods and Glacier Geohazards with Remote Sensing, MDPI - Multidisciplinary Digital Publishing Institute, 2021. doi:10.3390/books978-3-0365-0067-6.

[20] D. C. Bezanilla, J. S. Ramírez, A. de Alba Ávila, Estudio multitemporal de fragmentación de los bosques en la sierra fría, aguascalientes, méxico., Madera y Bosques 14 (2008) 37–51. URL: https://search.ebscohost.com/login.aspx?direct=true&AuthType=sso&db=fua&AN=35903269&lang=es&site=eds-live&scope=site&custid=s6026984.

[21] D. Armenteras, N. Rodríguez, DinÁmicas y causas de deforestaciÓn en bosques de latino amÉrica: Una revisiÓn desde 1990, Colombia Forestal 17 (2014) 233. URL: http://revistas.udistrital.edu.co/ojs/index.php/colfor/article/view/5382. doi:10.14483/udistrital.jour.colomb.for.2014.2.a07.

[22] A. Ariza, J. S. Rey, S. M. de Miguel, Comparison of maximum likelihood estimators and regression models for burn severity mapping in mediterranean forests using landsat tm and etm+ data., Revista Cartográfica (2019) 145–177. URL: https://search.ebscohost.com/login.aspx?direct=true&AuthType=sso&db=asn&AN=136455800&lang=es&site=eds-live&scope=site&custid=s602698410.35424/rcar.v5i98.145.

[23] Y. G. Ortega, D. V. Rivera, D. M. Castillo, Dinámica de la frontera agrícola del sistema de cuencas hidrográficas del zapotal mediante herramientas de teledetección, Ciencia y Tecnología 16 (2023) 12–23. URL: https://revistas.uteq.edu.ec/index.php/cyt/article/view/637. doi:10.18779/cyt.v16i1.637.

[24] G. Medina, A. Mejía, Análisis multitemporal y multifractal de la deglaciación de la cordillera parón en los andes de perú., Ecologia Aplicada 13 (2014) 35–42. URL: https://search.ebscohost.com/login.aspx?direct=true&AuthType=sso&db=eih&AN=97208990&lang=es&site=eds-live&scope=site&custid=s6026984. doi:10.21704/rea.v13i1-2.452.

[25] B. K. Veettil, S. F. R. Pereira, S. Wang, P. T. Valente, A. E. B. Grondona, A. C. B. Rondón, I. C. Rekowsky, S. F. D. Souza, N. Bianchini, U. F. Bremer, J. C. Simões, Un análisis comparativo del comportamiento diferencial de los glaciares en los andes tropicales usando teledetección, Investigaciones Geográficas (2016) 3. URL: https://investigacionesgeograficas.uchile.cl/index.php/IG/article/view/41215. doi:10.5354/0719-5370.2016.41215.

[26] B. Sánchez-Díaz, La teledetección en investigaciones ecológicas como apoyo a la conservación de la biodiversidad: una revisión, Revista científica 3 (2018) 243–253. URL: http://revistas.udistrital.edu.co/ojs/index.php/revcie/article/view/13370. doi:10.14483/23448350.13370.

[27] S. Malvina, C. G. Herrera, A. E. Niz, Teledetección aplicada al mapeo geomorfológico de los volcanes de la cuenca alta del río chaschuil, provincia de catamarca, argentina, Tecnura 23 (2019) 13–26. doi:10.14483/22487638.14642.

[28] R. V. Diñeiro, Seguimiento y clasificación de parámetros biofísicos de superficies agrícolas a partir de sensores remotos radar (2020). URL: https://search.ebscohost.com/login.aspx?direct=true&AuthType=sso&db=edsred&AN=edsred.10366.145429&lang=es&site=eds-live&scope=site&custid=s6026984.

[29] S. Liang, J. Cheng, J. Zhang, Maximum likelihood classification of soil remote sensing image based on deep learning, Earth sciences research journal 24 (2020) 357–365. doi:10.15446/esrj.v24n3.89750.

[30] M. Ramírez, L. Martínez, M. Montilla, O. Sarmiento, J. Lasso, S. Diaz, Obtención de coberturas del suelo agropecuarias en imágenes satelitales sentinel-2 con la inyección de imágenes de dron usando random forest en google earth engine, Revista de teledetección 2020 (2020) 49–68. doi:10.4995/raet.2020.14102.

[31] A. I. A. Huapaya, P. C. Sotelo, C. C. Benites, C. R. Philipps, G. V. Bejarano, Variación del Área Agrícola en el Distrito La Yarada Los Palos, Tacna, Perú., Espacio y Desarrollo (2020) 99–120. URL: https://search.ebscohost.com/login.aspx?direct=true&AuthType=sso&db=fua&AN=151638307&lang=es&site=eds-live&scope=site&custid=s602698410.18800/espacioydesarrollo.202001.004.

[32] J. Mejía-Marcacuzco, E. Pino-Vargas, E. Guevara-Pérez, V. Olivos-Alvites, M. Condori-Ventura, Predicción espacial de la erosión del suelo en zonas áridas mediante teledetección. estudio de caso: Quebrada del diablo, tacna, perú, Revista Ingeniería UC 28 (2021) 252–264. URL: https://www.revistas.uc.edu.ve/index.php/revinguc/article/view/24. doi:10.54139/revinguc.v28i2.24.

[33] F. Rahal, F.-Z. Baba-Hamed, Mapping of clay soils by remote sensing in the area of mers el kébir, algeria, Revista Facultad de Ingeniería Universidad de Antioquia (2022) 9. URL: https://revistas.udea.edu.co/index.php/ingenieria/article/view/344875. doi:10.17533/udea.redin.20221099.

[34] A. C. E. Zúñiga, J. C. Rodriguez, J. V. B. Saya, J. A. Ñaupari Vázquez, Estimación de la biomasa de una comunidad vegetal altoandina utilizando imágenes multiespectrales adquiridas con sensores remotos uav y modelos de regresión lineal múltiple, máquina de vectores soporte y bosques aleatorios, Scientia Agropecuaria 13 (2022). URL: https://search.ebscohost.com/login.aspx?direct=true&AuthType=sso&db=edsdoj&AN=edsdoj.4472aa60b05b49daa0d9cd963c9bc3d0&lang=es&site=eds-live&scope=site&custid=s6026984. doi:10.17268/sci.agropecu.2022.027.

[35] A. Ahmad, S. E. Noor, P. C. Cassinello, V. M. Núñez, Artificial intelligence (ai) as a complementary technology for agricultural remote sensing (rs) in plant physiology teaching., REiDoCrea: Revista Electrónica de Investigación y Docencia Creativa 11 (2022) 695–701. URL: https://search.ebscohost.com/login.aspx?direct=true&AuthType=sso&db=fua&AN=161802827&lang=es&site=eds-live&scope=site&custid=s6026984.

[36] M. Mulder, Monitoring land restoration projects of justdiggit in kenya, using downscaled passive microwave remote sensing products of vandersat (2018). URL: https://repository.tudelft.nl/islandora/object/uuid%3A86a24122-e3b5-4cc7-b580-f70fdecb78f8.

[37] L. Villani, G. Castelli, F. Sambalino, L. A. A. Oliveira, E. Bresci, Integrating uav and satellite data to assess the effects of agroforestry on microclimate in dodoma region, tanzania, 2020 IEEE International Workshop on Metrology for Agriculture and Forestry, MetroAgriFor 2020 - Proceedings (2020) 338–342. doi:10.1109/METROAGRIFOR50201.2020.9277643.

[38] M. V. der Vliet, R. D. Jeu, Y. Malbeteau1, D. Ghent, K. Veal, S. D. Haas, T. V. der Zaan, R. Sinha, S. Dash, R. Houborg, Quantifiable impact: monitoring landscape restoration from space (2023). URL: https://www.researchsquare.comhttps://www.researchsquare.com/article/rs-2669521/v1. doi:10.21203/RS.3.RS-2669521/V1.

[39] T. W. B. Group, Kenya - climatology | climate change knowledge portal, 2024. URL: https://climateknowledgeportal.worldbank.org/country/kenya/climate-data-historical.

[40] T. W. B. Group, Tanzania - climatology | climate change knowledge portal, 2024. URL: https://climateknowledgeportal.worldbank.org/country/tanzania/climate-data-historical.

[41] P. Sanchez, john Wiley, Suelos del trópico: características y manejo, Universidad Estatal de Carolina del Norte Raleigh, 1981.

[42] G. LLC, ImageCollection Visualization Google Earth Engine Google for Developers, 2024. URL: https://developers.google.com/earth-engine/guides/ic_visualization.

[43] L. A. N. de Aeronáutica y del Espacio NASA, Landsat 7 | landsat science, 2024. URL: https://landsat.gsfc.nasa.gov/satellites/landsat-7/.

[44] G. LLC, Landsat Collection 1 to Collection 2 migration Google Earth Engine Google for Developers, 2024. URL: https://developers.google.com/earth-engine/landsat_c1_to_c2.

[45] G. LLC, Imagecollection visualization google earth engine | google for developers, 2024. URL: https://developers.google.com/earth-engine/guides/ic_visualization.

[46] IDEAM, Formato común hoja metodológica (2024). URL: www.ideam.gov.co.
[47] G. LLC, Platform – Google Earth Engine, 2014. URL: https://earthengine.google.com/platform/.
[48] P. Refaeilzadeh, L. Tang, H. Liu, Cross-Validation, Springer New York, 2018, pp. 677–684. doi:10.1007/978-1-4614-8265-9_565.
[49] A. de la ONU para refugiados ACNUR, Emergencia por la sequía en el cuerno de África | acnur, 2024. URL: https://www.acnur.org/emergencias/cuerno-de-africa.
[50] A. de la ONU para refugiados ACNUR, El cuerno de África sufre la peor sequía de los últimos años, 2024. URL: https://eacnur.org/es/actualidad/noticias/desplazados/el-cuerno-de-africa-sufre-la-peor-sequia-de-los-ultimos-anos.
[51] J. T. Abatzoglou, S. Z. Dobrowski, S. A. Parks, K. C. Hegewisch, Terraclimate: Monthly climate and climatic water balance for global terrestrial surfaces, university of idaho earth engine data catalog | google for developers, 2018. URL: https://developers.google.com/earth-engine/datasets/catalog/IDAHO_EPSCOR_TERRACLIMATE#citations.